RSC Advances

ROYAL SOCIETY OF CHEMISTRY

www.rsc.org/advances

Cite this: DOI: 10.1039/c0xx00000x

www.rsc.org/xxxxxx

ARTICLE TYPE

Simultaneous determination of multicomponent in explosives using ultraviolet spectrophotometry and partial least square method

Tao Lu [a], Yuan Yuan [c], Xuan He [b], Menglong Li [a], Xuemei Pu [a,*], Tao Xu [b,*], Zhining Wen [a,*]

Received (in XXX, XXX) Xth XXXXXXXXX 20XX, Accepted Xth XXXXXXXXX 20XX
DOI: 10.1039/b000000x

The quantitative analysis of explosives is very important for national defence and security inspection. However, the conventionally analytical methods are complicated and time-consuming because of the complexity of the explosive samples. Herein, we proposed a new quantitative method, which combined ultraviolet (UV) spectrophotometry with partial least square regression (PLS-1 and PLS-2), to quickly determine the contents of 1,3,5,7-tetranitro-1,3,5,7-tetraazacyclo-octane (HMX), hexahydro-1,3,5-trinitro-1,3,5-triazine (RDX) and 2,4,6-trinitrotoluene (TNT) simultaneously from the mixed explosive samples. The calibration models were constructed by using 49 reference samples in the calibration set and optimized by the full cross-validation. The predictive performance of the optimized models was validated by the 21 explosive samples in an independent test set. The standard errors of prediction (SEP) were lower than 1.4 μg mL^{-1} for HMX, 2.2 μg mL^{-1} for RDX, and 0.8 μg mL^{-1} for TNT in both two PLS models. Finally, the optimized PLS-1 and PLS-2 models were successfully applied to simultaneously determine the three explosive ingredients in eight polymer bonded explosives (PBXs). The average recovery was close to 100% for each of the three components. Thus, UV spectrophotometry combined with the PLS regression can be considered as a promising strategy to conduct the determination of HMX, RDX and TNT in practice.

1. Introduction

2,4,6-trinitrotoluene (TNT), hexahydro-1,3,5-trinitro-1,3,5-triazine (RDX) and 1,3,5,7-tetranitro-1,3,5,7-tetraazacyclo-octane (HMX) are polynitro-explosives. Also, they are three of the most widely used secondary explosive ingredients in ammunition formulation and plastic explosives.[1-3] A majority of military explosives and commercial ones are highly filled with composite materials, which mainly contain one to three energetic compounds (*e.g*., HMX, RDX, TNT) as main components and a small quantity of organic compounds (*e.g*., waxes, stabilizers, plasticizers, oils) as fillers.[4] In recent years, the surge of explosive-based terrorisms have led to enormous damage to society.[5-8] Therefore, it is important for national defence and security inspection to identify the types of explosives rapidly and determined their contents accurately.

In the past decades, a great number of analytical methods have been developed in the field. The most common methods involve ion mobility spectrometry (IMS),[9-12] mass spectrometry (MS),[13-15] Raman spectroscopy,[5,16,17] THz spectroscopy,[18-20] laser induced breakdown spectroscopy (LIBS),[21-24] gas chromatography (GC),[25-27] high performance liquid chromatography (HPLC)[28-31] and some combined methods (*viz*. HPLC-MS[29] and GC-MS[32]). Although these instrumental techniques are highly selective and sensitive, most of the devices are rather bulky, expensive, and time-consuming,[33] impeding the quick and on-line determination. Thus, it is quite necessary to further develop new methods or improve the existing analytical techniques to enable faster, more sensitive, less expensive and simpler determinations to facilitate the determination of explosives.

As known, the ultraviolet (UV) spectrophotometry can easily and quickly conduct the quantitative analysis for a specific compound with high accuracy. However, they cannot be directly applied in the analysis of the military and commercial explosives because the multicomponents are involved in these explosives and some components have very similar physicochemical properties, leading to highly overlapped absorption bands in UV spectra.[34-36] Thus, the UV spectrophotometer has commonly been used as a detector in HPLC for the determination of explosives and other complicated samples.

Chemometrics was firstly introduced by Svan Wold[37] in 1972, which utilized mathematical and statistical approaches to design optimal steps in experiments and extracted maximal information from the experimental data.[38] Multivariate calibration methods in chemometrics play an important role in multicomponent resolution and quantification[34, 39-43] and have been successfully used to solve the problems existed in the spectral data of complicated mixtures, such as collinearity, band overlaps and interactions.[44-49] Partial least squares (PLS) regression initiated by Wold[50] has been successfully used in multicomponent quantitative analysis in many complicated cases.[39,51-55]The calibration of multiple response data by PLS can be performed via two methods, namely constructing multiple models with one response (*viz*., PLS-1) and building one model with multiple responses (*viz*., PLS-2).[56] The former executes the decomposition and regression for only single component at a time, while the latter calculates latent variables based on all of the components and only one calibration matrix is used.

Based on the considerations above, we, herein, combine the UV spectrophotometry with PLS algorithm to develop a new method to simultaneously determine the contents of HMX, RDX and TNT in the mixed explosives. We firstly construct the PLS-1 and PLS-2 models by using a well-designed calibration set, which included 49 reference samples with known proportions of HMX, RDX and TNT. Then, the models were validated by an independent test set. Finally, the optimized PLS models were applied to eight polymer bonded explosives. Satisfied results were obtained from the PLS models, indicating that it is highly potential for the UV spectrophotometry in combination with PLS to realize a simple, quick and accurate quantification determination on either the single-component explosives or the multicomponent ones.

2. Experimental

2.1. Chemical reagents and stock solutions

HMX, RDX, TNT and eight polymer bonded explosives (PBXs) based on the three analytes were provided by the Yinguang Chemical Plant, China. Analytical reagent grade acetonitrile was purchased from Chengdu Kelong Chemical Reagent Factory (Chengdu, China) and further purified. Stock solutions of 1014 μg mL^{-1} for HMX, 1002 μg mL^{-1} for RDX and 1010 μg mL^{-1} for TNT were prepared by dissolving appropriate amount of the analyte in acetonitrile and diluting to the mark with acetonitrile in 50 mL volumetric flasks.

2.2. Standard solutions and sample solutions

Stock solutions of HMX, RDX and TNT were utilized to construct the calibration set. These stock solutions were properly diluted to give work solutions with the concentration range of 0.81-32.45 μg mL^{-1} for HMX, 0.80-28.06 μg mL^{-1} for RDX, and 0.81-26.66 μg mL^{-1} for TNT. The calibration set consists of 49 samples, including 15 single-component mixtures, 9 binary-component mixtures and 25 ternary-component mixtures.

To validate the calibration models, an independent test set involved 21 samples with one to three components was randomly prepared using the same stock solutions with concentration inside the limits of the calibration set.

For the purpose of inspecting the predictive performance of the optimized PLS models in real cases, we validated the models by using eight real PBX samples. The real explosives were weighed and then powdered in a mortar. An appropriate amount of accurately weighed mixtures of the homogenous powder was dissolved with acetonitrile and then were filtered. 1.00 mL of this filtrate was diluted to 50.00 mL with acetonitrile.

2.3. Apparatus and software

Absorption spectra were recorded in a wavelength (λ) range of 190-400 nm at 1 nm intervals with respect to a blank of acetonitrile in a 1 cm quartz cell, using a Hitachi U-1900 UV-Vis spectrophotometer (Tokyo, Japan) with a scan fate of 400 nm/min and slit width 4.0 nm.

All data obtained from the experiments were gathered in a matrix data by Microsoft Office Excel (version 2010) and transferred to MATLAB software. All calculations were done using MATLAB (version 2013 a).

2.4. Procedures

2.4.1. Single component calibration

In order to find the linear concentration range of each material, single component calibrations were executed. Different volumes of the stock solution of each component was added to 10 mL volumetric flask and diluted to the mark with acetonitrile. The absorption spectra were recorded over 190-400 nm against a solvent blank. For each explosive, the linearity ranges were determined by plotting the absorbance at its λ_{max} (228 nm for HMX and TNT, and 197 nm for RDX) versus the sample concentration. The linear concentrations range from 0.41 μg mL^{-1} to 33.29 μg mL^{-1} for HMX, from 0.62 μg mL^{-1} to 29.12 μg mL^{-1} for RDX and from 0.29 μg mL^{-1} to 27.13 μg mL^{-1} for TNT. The characteristic parameters for the regression equations of individual calibrations were listed in Table 1.

Table 1. Parameters of the linear regression equations for each analyte.

Parameter	HMX (228 nm) [a]	RDX (197nm) [a]	TNT (228 nm) [a]
Linear range (μg mL^{-1})	0.41-33.29	0.62-29.12	0.29-27.13
Intercept	0.0087	0.0479	0.0411
Slope	68.966	64.038	81.460
Correlation coefficient	0.9992	0.9961	0.9992
LOD (μg mL^{-1}) [b]	0.27	0.33	0.23
LOQ (μg mL^{-1}) [c]	0.91	1.11	0.77

[a] The values in parenthesis correspond to the maximum absorption wavelength. [b] The LOD (limit of detection) was determined by a signal-to-noise ratio (S/N) = 3 for each analyte. [c] The LOQ (Limit of quantitation) was determined by a signal-to-noise ratio (S/N) = 10 for each analyte.

2.4.2. Multivariate calibration

In the determination of the three assayed explosive ingredients, the obtained spectral data were organized in an X matrix, in which each row stands for a given sample and each column corresponds to the absorbance value at a given wavelength. There are a total of 211 wavelengths in a spectrum. The concentration value of each of the three assayed explosives was utilized to compose the y vector. A full cross-validation was employed to construct optimum PLS models between the spectral data and the concentration values using the calibration set containing 49 reference samples. Then, the models were validated by an independent test set of 21 samples and 8 real polymer bonded explosives. In order to detect whether there are outliers in the calibration and independent test samples, the residual analysis [43,57,58] was executed in the PLS regression models.

3. Results and Discussion

Fig.1 shows the chemical structures of HMX, RDX and TNT and Fig.2 exhibits their corresponding absorbance spectra. As can be observed from Fig.2, the spectra of HMX, RDX and TNT are seriously overlapped, which prevents the direct determination by means of classical univariate calibration method without prior separation. Thus, it is necessary to use multivariate calibration techniques, such as PLS, to realize simultaneous determination of HMX, RDX and TNT in the mixed explosive samples.

Table 2. Concentration data (μg mL^{-1}) for the forty-nine samples in the calibration set.

Sample NO.	HMX	RDX	TNT	Sample NO.	HMX	RDX	TNT
Ternary mixtures				Binary mixtures			
1	0.81	0.80	0.81	26	-	0.80	7.27
2	0.81	8.02	7.27	27	-	8.02	13.74
3	0.81	15.23	13.74	28	-	15.23	20.20
4	0.81	22.44	20.20	29	-	22.44	26.66
5	0.81	28.06	26.66	30	0.81	28.06	-
6	8.11	0.80	7.27	31	17.04	15.23	-
7	8.11	8.02	13.74	32	32.45	0.80	-
8	8.11	15.23	20.20	33	8.11	-	0.81
9	8.11	22.44	26.66	34	25.15	-	13.74
10	8.11	28.06	0.81	Single component solutions			
11	17.04	0.80	13.74	35	0.81	-	-
12	17.04	8.02	20.20	36	8.11	-	-
13	17.04	15.23	26.66	37	17.04	-	-
14	17.04	22.44	0.81	38	25.15	-	-
15	17.04	28.06	7.27	39	32.45	-	-
16	25.15	0.80	20.20	40	-	0.80	-
17	25.15	8.02	26.66	41	-	8.02	-
18	25.15	15.23	0.81	42	-	15.23	-
19	25.15	22.44	7.27	43	-	22.44	-
20	25.15	28.06	13.74	44	-	28.06	-
21	32.45	0.80	26.66	45	-	-	0.81
22	32.45	8.02	0.81	46	-	-	7.27
23	32.45	15.23	7.27	47	-	-	13.74
24	32.45	22.44	13.74	48	-	-	20.20
25	32.45	28.06	20.20	49	-	-	26.66

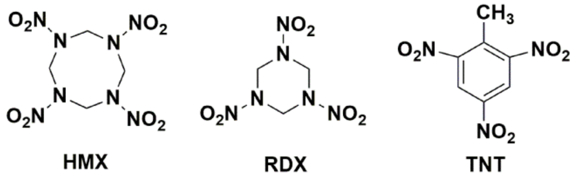

Fig. 1. Chemical structures of the three energetic compounds.

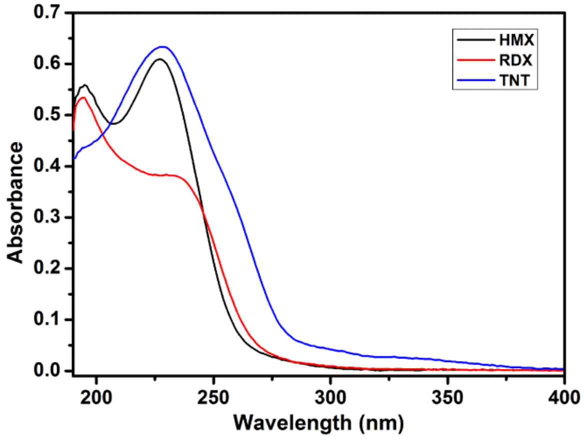

Fig. 2. Absorption spectra of 8.11 μg mL^{-1} HMX (black line), 8.02 μg mL^{-1} RDX (red line) and 7.27 μg mL^{-1} TNT (blue line).

3.1. The calibration set: construction of PLS models

3.1.1. Experimental design

Four important factors were considered in constructing the sample solution of the calibration set. Firstly, the concentration of each component must be in its linear range. Secondly, the concentration of the analyte in the calibration samples must be orthogonal in order to provide the maximal information of the studied system. Thirdly, the total absorbance of the standard mixture solutions was not beyond the maximum absorbance reading of the spectrophotometer (*i.e.* does not overload). Fourthly, the UV spectral data of the corresponding solutions were recorded in the same determination conditions. In the conditions, the ternary-component samples in the calibration set are constructed according to a five-level orthogonal array design (OAD, L_{25} (5^6)).[59] The binary-component and single-component samples are also prepared according to the same five concentration levels above. Table 2 lists the concentrations of the three analytes in the calibration set.

3.1.2. The selection of the number of factors and optimized PLS models

In order to avoid overfitting, it is of great importance to reduce the number of features and accurately select the optimal number of factors. Thus, a full cross-validation called leave-one-out cross-validation (LOO-CV) was utilized to tackle the problem in our study. The main principle of LOO-CV was to leave out one sample from the calibration set in each iteration and perform the PLS calibration with the remaining samples. Then, the concentration of the hold-out sample was predicted by the obtained PLS model. This procedure was iteratively repeated until each sample in the calibration set had been left out once. Then, the known concentrations of the analytes in each reference sample were compared with the prediction concentrations of the analytes in each sample and the standard error of cross-validation (SECV) was calculated in terms of Eq. (1).

$$\mathrm{SECV}=\left[\frac{1}{\mathrm{m}}\bullet\sum_{i=1}^{m}\left(C_{\mathrm{pred,i}}-C_{\mathrm{act,i}}\right)^{2}\right]^{1/2} \quad (1)$$

where $C_{\mathrm{pred,\ i}}$ is the predicted concentration of the interested component in i*th* mixture through the model, $C_{\mathrm{act,\ i}}$ is the real concentration, and *m* is the number of samples in the calibration set.

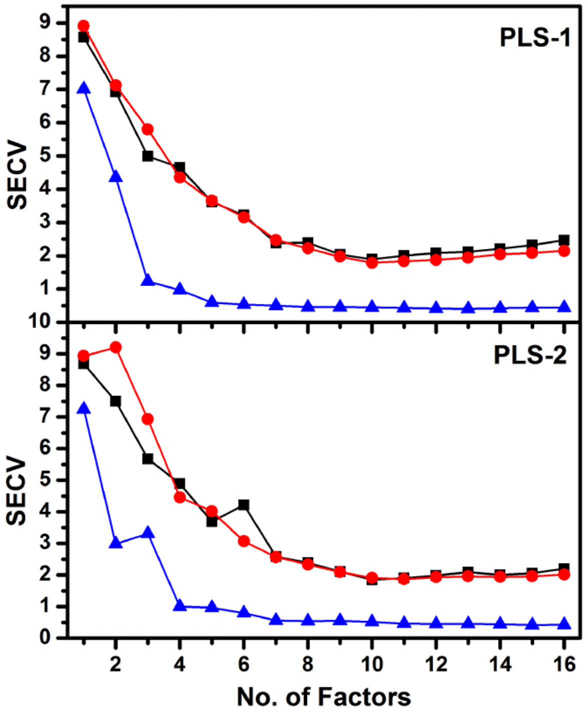

Fig. 3. Plot of standard error of cross-validation (SECV) vs the number of factors in the PLS-1 and PLS-2 calibration models for HMX (—■—), RDX (—●—) and TNT (—▲—).

To determine the optimum number of factors, the SECV value was calculated in the same way each time after a new factor was added to the models. The variation of SECV values with respect to the number of factors was shown in Fig. 3. It was required that the SECV value of the model with the optimum number of factors is not significantly greater than the minimal SECV. The F-statistic was used to make the significance determination by means of a comparison of the calculated F-value with the cutoff value (α=0.25), which was proposed to be a good criterion by Haaland and Thomas.[60] As a result, the optimum number of factors in the PLS-1 and PLS-2 models for HMX and RDX were determined to be 9. For TNT determination, the optimum number of factors are 10 for PLS-1 model and 14 for PLS-2 one. Table 3 lists the optimum number of factors selected, the standard error of calibration (SEC), standard error of cross-validation (SECV)，standard error of prediction (SEP) and the correlation coefficient of determination (R^2_{cal}) in the calibration set for each analyte. As can be seen from Table 3, the satisfactory results are obtained for all the analytes in PLS-1 and PLS-2 models, confirming the reliability of the two models constructed.

In addition, the outliers in the regression models were detected by using the residual analysis.[43,57,58] In general, a residual (ε_{i}) is defined as the difference between an experimental observation and a predicted value from a regression model, $\varepsilon_{\mathrm{i}} = y_{\mathrm{act,i}} - y_{\mathrm{pred,i}}$ where $y_{\mathrm{act,i}}$ is the real value and $y_{\mathrm{pred,i}}$ is the predicted value by the regression model. Fig. 4 shows that the residual values for the three components for the calibration samples in PLS-1 model. As can be seen from Fig.4, the residuals are scattered closely around the horizontal line, confirming that there are no outliers in the calibration samples and the regression model constructed is reliable. Similarly, the outliers have not been detected by the residual plot in PLS-2 model (see Fig. S1, ESI†).

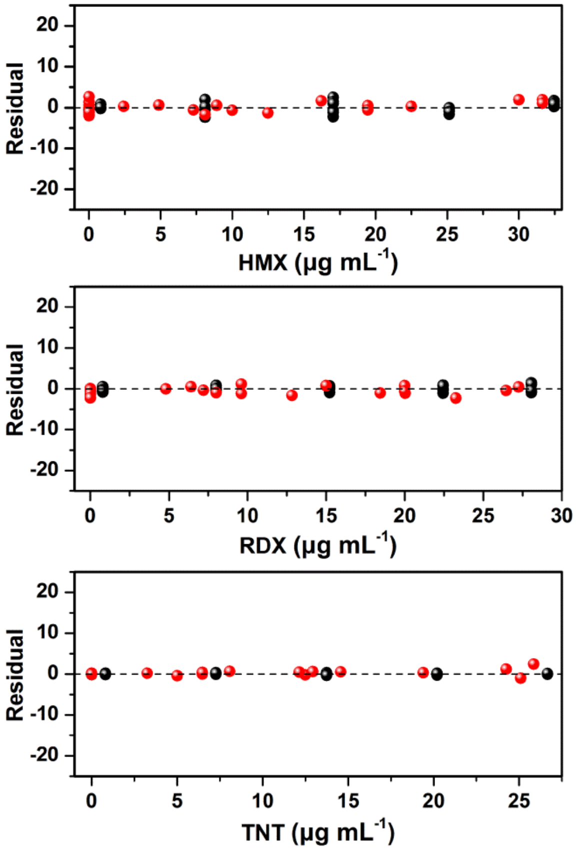

Fig. 4. Absolute residual distribution of PLS-1 model vs concentrations plots for the three components for the calibration (●) and independent test (●)samples.

3.2. Validation of the PLS Models by the independent test set

To validate the predictive performance of the optimized models, an independent test set of 21 samples containing 7 ternary-component samples, 8 binary-component samples and 6 one-component samples was prepared. The reference values of the explosive compositions are listed in the first three columns of Table 4. the constructed PLS-1 and PLS-2 models were used to estimate the contents of HMX, RDX and TNT in the independent test set and the results are listed in Table 4. As can be seen from Table 4, the estimated concentrations are close to the reference ones. Also, the residual analysis was carried out for the three components for the independent test samples in the PLS regression models (see Fig. 4 and Fig.S1). Similarly, no outliers were detected in the independent data set.

Table 3. Statistical parameters of the PLS-1 and PLS-2 models obtained from the calibration set.

	PLS-1					PLS-2				
	Factors[a]	SEC [b]	SECV [c]	SEP [d]	R^2_{cal}	Factors [a]	SEC	SECV	SEP	R^2_{cal}
HMX	9	1.2325	2.0428	1.2579	0.9898	9	1.3191	2.1097	1.371	0.9883
RDX	9	0.8285	1.9730	1.6706	0.9938	9	0.9488	2.0962	2.1091	0.9919
TNT	10	0.1331	0.4498	0.6959	0.9998	14	0.2168	0.4507	0.7787	0.9995

[a] The optimum number of factors. [b] Standard error of the calibration set. [c] Standard error of cross-validation. [d] Standard error of the independent test set.

Table 4. Determination of HMX, RDX and TNT (μg mL^{-1}) in the prediction set.

Reference values			Predicted values					
HMX	RDX	TNT	PLS-1			PLS-2		
			HMX	RDX	TNT	HMX	RDX	TNT
			Ternary mixtures					
22.50	15.00	5.00	22.27	14.23	5.37	22.68	14.80	5.67
12.50	20.00	12.50	13.82	19.26	12.70	14.42	20.02	12.98
8.92	26.45	25.10	8.37	26.87	26.08	9.68	28.59	26.61
16.22	9.62	12.14	14.58	10.80	11.71	15.14	11.45	11.98
31.64	23.25	19.39	29.70	26.55	19.08	30.33	27.37	18.93
19.47	8.02	6.48	18.99	8.95	6.09	19.29	9.13	6.02
7.30	9.62	6.48	7.91	8.49	6.48	8.03	8.49	6.43
			Binary mixtures					
30.01	-	12.93	28.08	1.42	12.36	28.02	1.76	12.69
19.47	-	6.48	20.10	-0.04	6.16	20.48	0.28	6.04
-	20.04	14.57	1.12	21.12	14.03	1.92	22.13	14.20
-	18.44	8.08	0.02	19.49	7.45	0.64	20.35	7.60
-	12.83	24.24	1.96	14.46	23.02	2.61	15.45	22.91
8.11	6.41	-	9.81	5.91	0.03	10.01	6.31	-0.07
10.00	20.00	-	10.65	20.56	-0.23	11.34	21.50	-0.24
2.43	7.21	-	2.14	7.55	-0.07	2.27	7.77	-0.09
			Single-component solutions					
4.87	-	-	4.31	0.20	0.02	4.16	-0.01	-0.03
31.64	-	-	30.60	1.44	-0.19	31.36	2.51	-0.19
-	4.81	-	-0.59	4.87	0.07	-0.77	4.62	0.08
-	27.25	-	1.06	26.80	0.02	1.74	27.79	0.19
-	-	3.24	-1.31	1.18	3.06	-1.40	1.05	3.06
-	-	25.86	-2.62	2.23	23.44	-2.22	2.37	23.26

Table 5 lists the correlation coefficient of determination (R^2_{pred}) and standard error of prediction (SEP) in the independent prediction set. As shown in Table 5, SEP values are lower than 1.4 for HMX，2.2 for RDX, and 0.8 for TNT. R^2_{pred} values are higher than 0.98 for the three components. In addition, the recovery rates obtained by PLS-1 were 99.33% for HMX, 102.82% for RDX and 97.21% for TNT. The recovery rates obtained by PLS-2 were 102.63% for HMX, 106.57% for RDX and 98.11% for TNT. These results demonstrated that the constructed PLS-1 and PLS-2 models have high predictive ability for simultaneous determination of HMX, RDX and TNT in the mixtures.

3.3. Application of the optimized models to the real samples

In order to test the applicability of the proposed methods to the real samples, the optimized PLS models were further used to simultaneously determine HMX, RDX and TNT in real explosive samples. Eight real PBX samples (three replicates per sample) were prepared as we describe in the experimental section above. The results derived from the PLS-1 and PLS-2 models were summarized in Table 6. As can be observed, the obtained results are satisfactory with a good recovery yield in general (average values of 101.19%, 95.27% and 95.42% in PLS-1 model, of 102.12%, 96.24% and 93.38% in PLS-2 model for HMX, RDX and TNT, respectively). The result indicates that our proposed methods are adaptable to simultaneously determine HMX, RDX and TNT in the real explosives. Thus, the UV-spectrum combined with chemometrics method should be highly potential to be a simple, quick and accurate analysis method in the explosive determination.

Table 5. A summarization in the predictive performances of the constructed PLS-1 and PLS-2 models for the independent prediction set.

Parameters	HMX		RDX		TNT	
	PLS-1	PLS-2	PLS-1	PLS-2	PLS-1	PLS-2
SEP	1.2579	1.3710	1.6706	2.1091	0.6959	0.7787
R^2_{pred}	0.9879	0.9852	0.9869	0.9841	0.9953	0.9930
Recovery (%) [a]	99.33	102.63	102.82	106.57	97.21	98.11

[a] The value is mean recovery for each component. Recovery (%) = 100 × ($C_{\mathrm{pred}}/C_{\mathrm{act}}$), C_{pred} represents the prediction concentration, C_{act} represents the actual concentration.

Table 6. Determination of HMX, RDX and TNT in the eight real explosive samples (μg mL^{-1}).

Reference values			Predicted values [a]					
HMX	RDX	TNT	PLS-1			PLS-2		
			HMX	RDX	TNT	HMX	RDX	TNT
Comp.A5								
-	10.50	-	-0.99	9.86	0.21	-1.25	9.40	0.28
Tritonal								
-	-	12.12	-1.41	1.67	10.95	-1.17	1.32	10.92
X-2042								
18.44	-	-	20.05	-0.91	-0.03	20.90	0.25	0.06
Comp.B-2								
-	7.42	4.94	-0.04	6.78	4.60	-0.28	6.52	4.71
Cyclotol								
-	8.56	3.76	-0.21	7.75	3.75	-0.57	7.29	3.83
LX-14								
19.30	-	0.38	18.62	0.64	0.37	18.00	0.73	0.35
PBX-71								
9.76	9.60	-	8.85	10.00	-0.08	8.91	10.07	-0.06
PBX-T-1								
13.50	9.06	6.06	14.37	8.73	5.85	14.93	9.43	5.91

[a] The average values of the three independent determinations.

Com. A5 (99% RDX and 1% stearic acid), Tritonal (80% TNT and 20% Aluminium powder)，X-2042 (92% HMX and 8% polymer), Comp. B-2 (60% RDX and 40% TNT), Cyclotol (70% RDX and 30% TNT) , LX-14 (95.9% HMX, 1.9 % TNT and 2.2% polymer), PBX-71 (49% HMX, 48% RDX ,1.5% F2311 and 1.5% F2314) and PBX-T-1(45% HMX, 30%RDX, 20%TNT and 5% Ammonium nitrate).

4. Conclusions

In this work, we have successfully applied the partial least square (PLS) regression to simultaneously determine the contents of HMX, RDX and TNT from the single-component, binary-component and ternary-component explosive samples, based on their UV spectra. Multivariate calibration models were built from the raw spectral data matrices of the calibration set using PLS-1 and PLS-2 methods and further verified through the independent test set of the explosive mixtures. Finally, eight real polymer bonded explosives were used to check the applicability of the models. The results showed that the contents of HMX, RDX and TNT in the mixed explosives can be satisfactorily estimated by our proposed method, indicating that it is feasible for UV spectrophotometry in combination with chemometric techniques to develop a simple, quick and reliable analysis method to realize simultaneous multicomponent determination on explosives.

Acknowledgements

This project is supported by the National Science Foundation of China (Grant No. U1230121 and 21273154).

Notes

[a] *College of Chemistry, Sichuan University, Chengdu 610064, People's Republic of China .Tel.: +86-028-85412290; Fax: +86-028-85412290; Email address：xmpuscu@scu.edu.cn*
[b] *Institute of Chemical Materials, Chinese Academy of Engineering Physics, Mianyang 621900, People's Republic of China*
[c] *College of Management, Southwest University for Nationalities, Chengdu 610041, People's Republic of China*

† Electronic Supplementary Information (ESI) available: [details of any supplementary information available should be included here]. See DOI: 10.1039/b000000x/

References

1 S. Babaee and A. Beiraghi, *Anal. Chim. Acta*., 2010, **662**, 9-13.
2 T. Lo, I. S. Gregory, C. Baker, P. F. Taday, W. R. Tribe and M. C. Kemp, *Vib. Spectrosc*., 2006, **42**, 243-248.
3 D. J. Funk, F. Calgaro, R. D. Averitt, M. L. T. Asaki and A. J. Taylor, *Appl. Spectrosc*., 2004, **58**, 428-431.
4 X. Cetó, A. M. O' Mahony, J. Wang and M. Del Valle, *Talanta*, 2013, **107**, 270-276.
5 M. López-López and C. García-Ruiz, *Trend. Anal. Chem*., 2014, **54**, 36-44.
6 R. J. Colton and J. N. Russell, *Science*, 2003, **299**, 1324-1325.
7 A. Fainberg, *Science*, 1992, **299**, 1531-1537.
8 S. F. Hallowell, *Talanta*, 2001, **54**, 447-458.
9 C. G. Fraga, D. R. Kerr and D. A. Atkinson, *Analyst*, 2009, **134**, 2329-2337.
10 D. S. Moore, *Sensing and Imaging*., 2007, **8**, 9-38.
11 G. A. Buttigieg, A. K. Knight, S. Denson, C. Pommier and M. Bonner Denton, *Forensic. Sci. Int*., 2003, **135**, 53-59.
12 T. L. Buxton and P. D. B. Harrington, *Anal. Chim. Acta*., 2001, **434**, 269-282.
13 J. J. Brady, E. J. Judge and R. J. Levis, *Rapid. Commun. Mass. Spectrom*., 2010, **24**, 1659-1664.
14 J. F. Garcia-Reyes, J. D. Harper, G. A. Salazar, N. A. Charipar, Z. Ouyang and R. G. Cooks, *Anal. Chem*., 2011, **83**, 1084-1092.
15 K. Sovová, K. Dryahina, P. Španěl, M. Kyncl and S. Civiš, *Analyst*, 2010, **135**, 1106-1114.
16 J. C. Carter, S. M. Angel, M. Lawrence-Snyder, J. Scaffidi, R. E. Whipple and J. G. Reynolds, *Appl. Spectrosc*., 2005, **59**, 769-775.
17 C. Eliasson, N. A. Macleod and P. Matousek, *Anal. Chem*., 2007, **79**, 8185-8189.
18 H. B. Liu and Y. Q. Chen, *Opt. Express*., 2006, **14**, 415-423.
19 J. Chen, Y. Q. Chen, H. W. Zhao, G. J. Bastiaans and X. C. Zhang, *Opt. Express*., 2007, **15**, 12060-12067.
20 M. R. Leahy-Hoppa, M. J. Fitch and R. Osiander, *Anal. Bioanal. Chem*., 2009, **395**,247-257.
21 J. L. Gottfried, F. C. De Lucia, Jr, C. A. Munson and A. W. Miziolek, *J. Anal. At. Spectrom*., 2008, **23**, 205-216.
22 J. L. Gottfried, F. C. De Lucia, Jr, C. A. Munson and A. W. Miziolek, *Anal. Bioanal. Chem*., 2009, **395**, 283-300.
23 J. Moros, J. Serrano, C. Sánchez, J. Macías and J. J. Laserna, *J. Anal. At. Spectrom*., 2012, **27**,2111-2122.
24 S. Sunku, M. K. Gundawar, A. K. Myakalwar, P. P. Kiran, S. P. Tewari and S. V. Rao, *Spectrochimica. Acta. B*., 2013, **79-80**, 31-38.
25 S. A. Barshick and W. H. Griest, *Anal. Chem*., 1998, **70**, 3015-3020.
26 M. Nambayah and T. I. Quickenden, *Talanta*, 2004, **63**, 461-467.
27 C. J. Miller, G. Elias, N. C. Schmitt and C. Rae, *Sensing and Imaging*., 2010, **11**, 61-75.
28 T. F. Jenkins, D. C. Leggett, C. L. Grant and C. F. Bauer, *Anal. Chem*., 1986, **58**, 170-175.
29 D. Gaurav, A. K. Malik and P. K. Rai, *Crit. Rev. Anal. Chem*., 2007, **37**, 227-268.
30 Gaurav, A. K. Malik and P. K. Rai, *J. Hazard. Mater*., 2009, **172**, 1652-1658.
31 P. Bansal, Gaurav, Nidhi, A. K. Malik and F. M. Matysik, *Chromatographia*, 2012, **75**, 739-745.
32 J. Yinon and S. Zitrin, John Wily & Sons Ltd, West Sussex, England, 1993.
33 L. Senesac and T. G. Thundat, *Mater. Today*., 2008, **11**, 28-36.
34 T. Azzouz and R. Tauler, *Talanta*, 2008, **74**,1201-1210.
35 C. B. Ojeda and F. S. Rojas, *Anal. Chim. Acta*., 2004, **518**, 1-24.
36 J. Kapinska, *Talanta*, 2004, **64**, 801-822.
37 B. Lavine and J. Workman, *Anal. Chem*., 2008, **80**, 4519-4531.
38 J. W. Einax, *Anal. Bioanal. Chem*., 2008, **390**, 1225-1226.
39 E. Dinc, D. Baleanu, G. Ioele, M. De Luca and G. Ragno, *J. Pharm. Biom. Anal*., 2008, **48**, 1471-1475.
40 M. De Luca, G. Ioele, A. Risoli and G. Ragno, *Microchem. J*., 2006, **83**, 24-34.
41 H. D. Li, Y. Z. Liang, Q. S. Xu and D. S. Cao, *Anal. Chim. Acta*., 2009, **648**, 77-84.
42 Z. C. Liu, W. S. Cai and X. G. Shao, *Analyst*., 2009, **134**, 261-266.
43 J. C. L. Alves and R. J. Poppi, *Analyst*, 2013, **138**, 6477-6487.
44 H. Martens and T. Naes, *Multivariate Calibration*, vol.7, Wiley, Chichester, 1989.
45 Y. N. Ni and X. F. Gong, *Anal. Chim. Acta*., 1997, **354**, 163-171.
46 B. Hemmateenejad, R. Ghavami, R. Miri and M. Shamsipur, *Talanta*, 2006, **68**, 1222-1229.
47 X. G. Shao, X. H. Bian and W. S. Cai, *Anal. Chim. Acta*., 2010, **666**, 32-37.
48 R. Ergon, *Chemom. Intell. Lab. Syst*., 2006, **81**,68-73.
49 J. F. Nie, H. L. Wu, X. M. Wang, Y. Zhang, S. H. Zhu and R. Q. Yu, *Anal. Chim. Acta*., 2008, **628**, 24-32.
50 H. Wold, in: H. Joreskog and H. Wold (Eds), Systems Under Indirect Observation, North-Holland, Amsterdam, 1982.
51 G. Ragno, G. Ioele and A. Risoli, *Anal. Chim. Acta*., 2004, **512**,173-180.
52 Y. H. Yuan, Y. Z. Liang, G. X. Xie, H. D. Li, D. S. Cao, Q. S. Xu, *Analyst*, 2013, **138**, 6412-6421..
53 J. El Haddad, F. de Miollis, J. Bou Sleiman, L. Canioni, P. Mounaix and B. Bousquet, *Anal. Chem*., 2014, **86**, 4927-4933.
54 D. Chen, W. S. Cai and X. G. Shao, *Anal. Chim. Acta*., 2007, **598**,19-26.
55 J. El Haddad, B. Bousquet, L. Canioni and P. Mounaix, *Trend. Anal. Chem*., 2013, **44**, 98-105.
56 J. P. Andries, Y. V. Heyden and L. M. Buydens, *Anal. Chem*., 2013, **85**, 5444-5453.
57 M. del Olmo, C. Díez, A. Molina, I. de Orbe and J. L. Vílchez, *Anal. Chim. Acta*., 1996, **335**, 23-33.
58 R.B. Keithley, M.L. Heien and R.M. Wigheman, *Trend. Anal. Chem*., 2009, **28**, 1127-1136.
59 X. L. Cheng, J. Y. Wan, P. Li and L. W. Qi, *J. Chromatogr. A*., 2011, **1218**, 5774-5786.
60 D. M. Haaland and E. V. Thomas, *Anal. Chem*., 1988, **60**, 1193-1202.

Graphical abstract

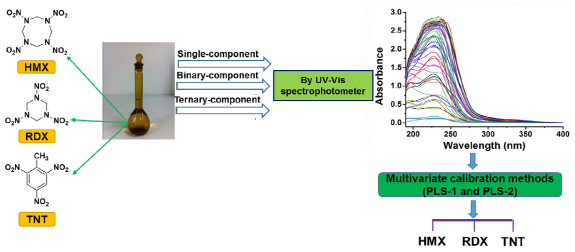

We used UV spectrophotometry and chemometrics method to develop a novel method for simultaneous multi-component determination in explosives.